Available online at www.sciencedirect.com
SCIENCE DIRECT
Chemical Physics 325 (2006) 129–137
Chemical Physics
www.elsevier.com/locate/chemphys

Doping-induced realignment of molecular levels at organic–organic heterojunctions

Antoine Kahn [a,*], Wei Zhao [a], Weiying Gao [b], Hector Vázquez [c], Fernando Flores [c]

[a] Department of Electrical Engineering, Princeton University, Olden Street, Princeton NJ 08544, USA
[b] DuPont Experimental Station, Wilmington, DE 19880-0356, USA
[c] Departamento de Física Teórica de la Materia Condensada, Universidad Autónoma de Madrid, E-28049 Madrid, Spain

Received 1 June 2005; accepted 13 September 2005
Available online 25 October 2005

Abstract

This article examines how the concept of alignment of charge neutrality levels (CNL) can be used to explain and predict interface dipole and molecular level offset at organic–organic (OO) heterojunctions. The application of the model of CNL alignment to interfaces between undoped materials is reviewed first. The model is then extended to explain the shift of the CNL upon electrical doping of an organic material, and the resulting change in interface dipole and molecular level alignment. This approach provides, at this point, the first comprehensive prediction of energetics at OO heterojunctions.

Keywords: Organic semiconductors; Heterojunctions; Molecular level alignment; Charge neutrality level

1. Introduction

Relative positions of molecular levels across metal–organic semiconductor (MO) and organic–organic semiconductor (OO) interfaces are key characteristics of organic thin film devices. Molecular level offsets define energy barriers that control carrier injection into, and transport between, layers. These barriers have a direct impact on the performance of organic devices like OFETs, OLEDs and photovoltaic cells. Understanding interface mechanisms and predicting energy level alignments is therefore highly relevant to engineering new devices and designing new functionalities.

Molecular level alignment at MO interfaces has been extensively investigated over the past decade [1–8]. Interfaces formed between spun-on polymer films and metallic surfaces have generally been found to approach the Schottky–Mott limit with near vacuum level alignment across the interface [9]. For these systems, charge injection barriers can therefore be fairly accurately predicted from the difference between the metal work function and the polymer ionization energy (for holes) or electron affinity (for electrons). On the other hand, vacuum evaporation of molecular films on clean metal surfaces, which presumably form interfaces where the molecule–metal interaction is more intimate than with spun-on films, has been shown experimentally to produce interfaces that depart from that limit and exhibit substantial interface dipoles Δ [1,3,8]. Several mechanisms have been proposed to explain the formation of these dipoles and MO barriers. At reactive interfaces, for example, the electronic structure can be entirely dominated by chemistry-induced gap states, which control the charge exchange between the two materials, determine the interface dipole Δ, pin the Fermi level in the gap of the organic material and define the barrier [10]. At unreactive interfaces, contributions to the vacuum level misalignment range from direct charge exchange between metal and molecule [5], reduction in metal work function caused by the adsorption of molecules [4,11,12], mirror charge in the metal substrate [4], and alignment of intrinsic molecular

* Corresponding author. Tel.: +1 609 258 4642; fax: +1 609 258 6279.
E-mail address: kahn@princeton.edu (A. Kahn).

0301-0104/$ - see front matter © 2005 Elsevier B.V. All rights reserved.
doi:10.1016/j.chemphys.2005.09.015

dipole moments [4]. Recently, a more general model based on the concept of induced density of interface states (IDIS) was developed to predict trends in barrier vs. metal work function and organic parameters [13,14]. In its original form, this and similar models were put forth 30 years ago to explain the formation of energy barriers at interfaces between metals and inorganic semiconductors [15–19]. According to the IDIS model, the continuum of metallic states in close proximity with the semiconductor induces a density of states in the organic gap. These states play a key role in defining the position of the Fermi level, and their occupation determines the size and sign of the interface dipole. Both Fermi level position and dipole depend on the density of induced gap states, on the position of the charge neutrality level (CNL) of these states, and on the relative positions of the metal Fermi level and CNL [18,19]. The degree of Fermi level pinning is generally expressed in metal-semiconductor physics in terms of the interface parameter S, which is defined as the change in Fermi level position in the gap of the semiconductor (E_F), equal to the negative of the change in electron injection barrier (Φ_{Bn}), as a function of the metal work function (Φ_M):

$$S = \frac{dE_F}{d\Phi_M} = -\frac{d\Phi_{Bn}}{d\Phi_M}. \quad (1)$$

Alternatively, S is defined in terms of the metal electronegativity [20], which avoids the problem of the high sensitivity of Φ_M to the specific state of the metal surface. S is naturally inversely related to the density of interface-induced states. The IDIS model was recently applied in the weak chemical interaction limit to interfaces between Au and several molecules like perylenetetracarboxylic-dianhydride (PTCDA) [13], 3,4,9,10-perylenetetracarboxylic bisbenzimidazole (PTCBI) [14], and 4,4′,*N*,*N*′-dicarbazolyl biphenyl (CBP) [14] (Fig. 1). Remarkably, the calculations concluded to IDIS of the order of $\sim 5\times10^{13}$–2×10^{14} eV^{-1} cm^{-2} for these interfaces, with the largest value (for PTCDA) comparable to IDIS calculated for Si or GaAs [19], and the smallest (for CBP) corresponding to materials with weaker pinning behavior and larger S-parameter. The model was shown to correctly predict trend and sign of MO interface S-parameters, dipoles Δ and injection barriers.

The IDIS model was recently extended to OO heterojunctions [21]. Photoemission studies done on a number of these systems in the past few years have shown that a majority of OO heterojunctions nearly follow vacuum level alignment, interface dipole Δ ($\leqslant$0.1 eV) [22–25]. However, a small number of these OO interfaces were found to exhibit a significant dipole, for example $\Delta = -0.5$ eV for PTCDA/tris(8-hydroxy-quinoline)aluminum (Alq_3) [26] and $\Delta = 0.4$ eV for copper phthalocyanine (CuPc)/PTCDA [27]. While previous analyses had not been able to resolve these differences and could not provide adequate predictions of molecular level alignment, the application of the IDIS model was found to provide an interesting opening based on the concept of alignment of the CNLs of the two organic materials [21].

Following a short experimental section on the formation of OO heterojunctions and measurement of molecular level offsets, we re-examine experimental results obtained for OO heterojunctions and give an account of the analysis and its application to the prediction of molecular level alignment. We show how the presence or absence of an interface dipole is rationalized in all cases. The second part of the paper considers the puzzling change in molecular level alignment induced by doping one of the constituents of the OO interface [28]. We show how (p-)doping actually shifts the CNL of doped organic materials, and how the IDIS model accounts for the realignment of molecular levels across the interface. Note that electrical doping in molecular solids involves the incorporation of a relative density of molecular dopants (0.1–1%) that is far larger than for standard inorganic semiconductor doping. Such concentration in inorganic semiconductors would normally lead to conditions beyond degenerate doping and associated with the formation of an alloy. In the case of (mostly amorphous) van der Waals-bonded molecular films, however, intermolecular overlap of wavefunctions is small and localization of carriers is strong, preventing the formation of doping-induced bands and similar phenomena associated with degenerately doped inorganic semiconductors. It is therefore generally accepted that the notion of doping remains valid, even with the very high concentrations of dopants mentioned above.

2. Experimental procedures

All the experiments were performed in ultra-high vacuum, using organic materials pre-purified by gradient sublimation techniques. OO heterojunctions were prepared by depositing 60–100 Å of one organic material on a substrate, typically Si(1 0 0): 200 Å Cr: 800 Å Au, then building the interface by incremental deposition of the second organic material on top of the first. At each step of the deposition, the position of the vacuum level, the valence states and the ionization energy (IE) of the film were measured by ultra-violet photoemission spectroscopy (UPS). Measurements were carried out until all contributions from the bottom organic film were eliminated and the valence level positions and line shapes of the overlayer film were saturated, signifying completion of the heterojunction. The resolution of the UPS measurements, performed with a He discharge lamp (HeI, 21.22 eV and HeII 40.84 eV) and a double-pass cylindrical mirror analyzer, was 0.15 eV. All IEs and energies of molecular levels were found to be reproducible ±0.1 eV.

For each interface, the interface dipole Δ, i.e. the shift of the vacuum level across the interface, was measured from the shift of the photoemission onset at the initial stage of overlayer deposition [26]. The offset between the highest occupied molecular orbitals (HOMO) for each OO hetero-

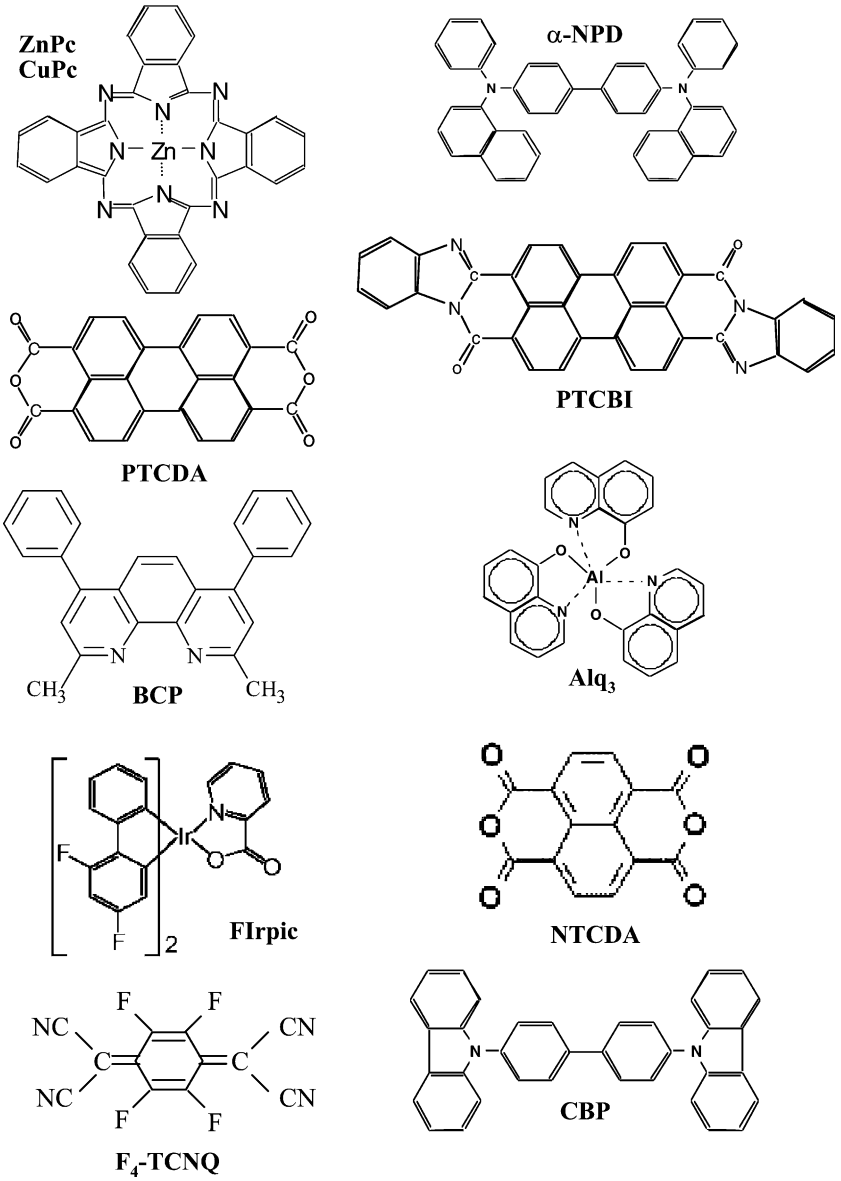

Fig. 1. Chemical structure of organic compounds mentioned in this article.

junction was defined as the energy difference between the linear extrapolation of the leading (low binding energy) edge of the HOMO peak on each side of the interface. The position of the lowest unoccupied molecular orbital (LUMO) of each material, and their offset across the interface, were deduced from the HOMO positions, adding in each case the transport gap previously determined by UPS and inverse photoemission spectroscopy (IPES) [29,30].

The doped films were made by co-evaporation of host and dopant [28,31–33]. The dopant used in this study was the strong electron-acceptor molecule tetrafluorotetracyanoquinodimethane (F_4-TCNQ), which has been shown to efficiently p-doped hole-transport materials like zinc phthalocyanine (ZnPc) [31,32] and *N*,*N*′-diphenyl-*N*,*N*′-bis(1-naphthyl)-1,1′-biphenyl-4,4′-diamine (α-NPD) [33].

3. Results and discussion

3.1. Undoped OO heterojunctions

The UPS spectra for the formation of a typical OO heterojunction, i.e. zinc phthalocyanine (ZnPc)/CBP, are shown in Fig. 2(a). From the point of view of the electronic structure of the heterojunction, the most important aspects of these spectra are the shift of the vacuum level across the interface, which denotes the interface dipole Δ, and the energy offset between the HOMOs of the two materials. In this particular case, $\Delta \leqslant 0.1$ eV and the HOMO–HOMO offset is 0.92 eV. Using the transport gaps previously determined by UPS/IPES for ZnPc [31] and CBP [28], one obtains the complete interface energy diagram, including LUMO–LUMO offset, displayed in Fig. 2(b). UPS spectra of a heterojunction with strong interface dipole are shown

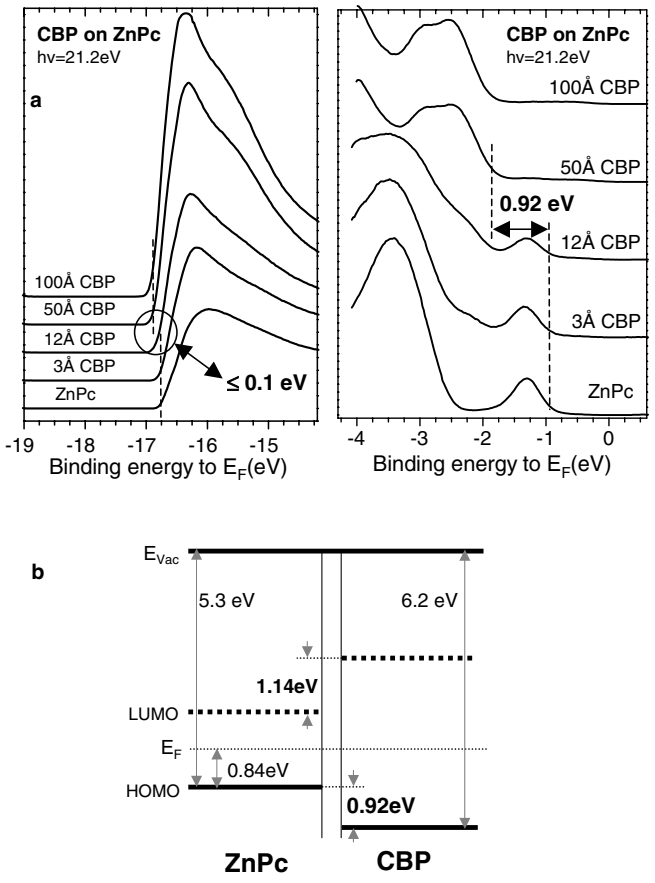

Fig. 2. (a) UPS spectra as a function of incremental deposition of CBP on ZnPc. The right panel shows the features corresponding to the frontier orbitals, with the ZnPc HOMO at 1.25 eV below E_F. The ZnPc/CBP HOMO–HOMO offset is 0.92 eV. The left panel shows the onset of photoemission. The absence of significant shift (<0.1 eV) upon deposition of 3 and 12 Å CBP indicates vacuum level alignment; (b) corresponding heterojunction energy diagram. The interface dipole is within experimental error of 0: $\Delta \leqslant 0.1$ ev.

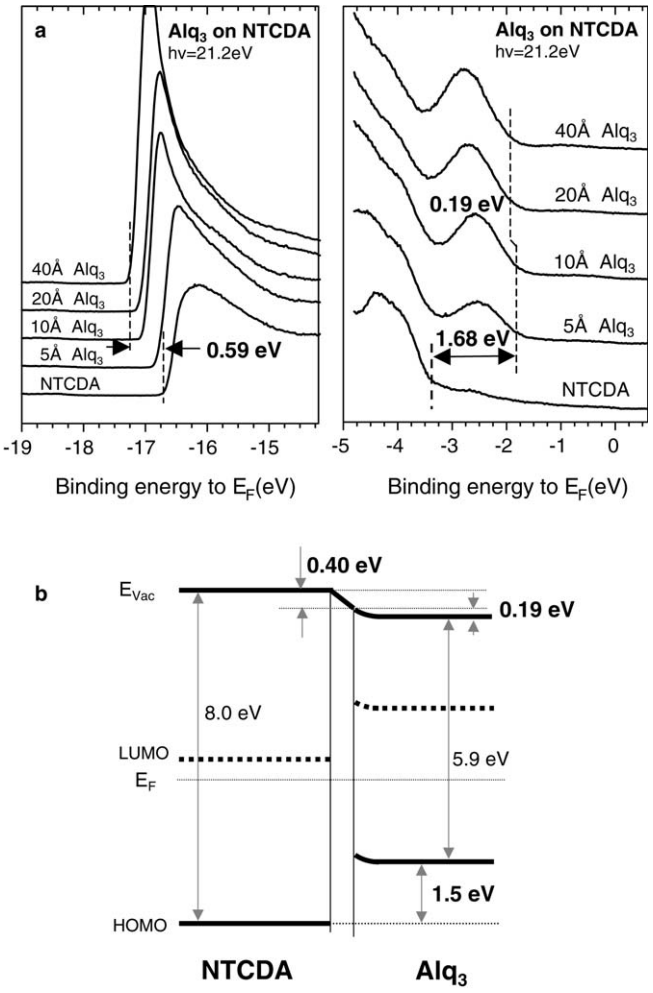

Fig. 3. Same as Fig. 2 for the NTCDA/Alq_3 heterojunction. The shift of the photoemission onset shows a −0.40 eV interface dipole.

in Fig. 3(a). In this case, a 0.4 eV shift in the onset of photoemission is measured upon deposition of the first molecular layers of Alq_3 on a film of 1,4,5,8-naphthalene-tetracarboxylic-dianhydride (NTCDA). The interface energy diagram is given in Fig. 3(b). It shows a −0.40 eV interface dipole and a 0.19 eV additional shift of the vacuum level and molecular levels. The latter is attributed either to the completion of the interface dipole upon formation of a continuous Alq_3 layer (the morphology of the interface is not known at the molecular level) or to a small amount of molecular level bending present if the layer has a small density of defects or impurities. Table 1 summarizes the experimentally determined Δ's of several undoped OO heterojunctions. Δ is chosen positive when the vacuum level increases (steps up) from the first organic listed in the heterojunction to the second The HOMO–HOMO offset can be deduced from the Δ's and the IE of each organic material (Table 2).

According to the IDIS model, the energetics of an OO barrier is controlled by charge transfer between the two organic semiconductors, the sign and magnitude of which are determined mainly by the energy difference between the initial positions of the CNLs of the two materials. The sign and magnitude of the interface dipole Δ reflect the sign

Table 1
Experimentally measured vs. calculated interface dipole for a number of OO heterojunctions

	Δ(experiment)	Δ(theory)
CuPc/PTCDA	0.4	0.43
CuPc/PTCBI	0.1	0.22
CuPc/CBP	0.0	0.09
CuPc/α-NPD	0.0	0.09
PTCDA/Alq_3	−0.5	−0.42
PTCDA/α-NPD	−0.1	−0.24
BCP/Alq_3	0.0	0.0
BCP/CBP	0.0	0.12
BCP/PTCBI	0.4	0.24
BCP/α-NPD	0.0	0.12
Alq_3/α-NPD	0.25	0.14
Alq_3/CBP	0.1	0.14
NTCDA/Alq_3	−0.4	−0.37
NTCDA/CuPc	−0.4	−0.38
NTCDA/BCP	−0.45	−0.32
FIrpic/Alq_3	−0.25	–

Results for several of these heterojunctions were published in [21].

Table 2
E_{CNL}: CNL position relative to E_{vac}; IE: ionization energy measured as the energy difference between E_{vac} and the centroid (the edge) of the HOMO peak; ε: dielectric constant of the material, calculated as defined in the text

	$-E_{CNL}$ (eV)	IE (eV)	ε
PTCDA	4.8	7.3 (6.8)	1.9
PTCBI	4.4	6.7 (6.2)	2.0
CBP	4.2	6.8 (6.25)	1.5
CuPc	4.0	5.7 (5.2)	2.5
α-NPD	4.2	6.0 (5.5)	1.5
BCP	3.8	6.9 (6.4)	1.4
Alq_3	3.8	6.3 (5.8)	1.6
NTCDA	4.8	8.5 (8.0)	1.6
FIrpic	–	6.7 (6.2)	1.6

and magnitude of the charge exchanged between the two materials. Accordingly, the CNL can be considered as playing a role analogous to that of the electronegativity of the material. The lower the CNL is in the gap of the (organic) semiconductor, the stronger is the attraction of this material for electronic charges. Given that the potential offset between two solid surfaces is screened according to the dielectric properties of the materials, the interface dipole that arises from the potential difference and charge exchange can be written as [21]

$$\Delta = (1 - S_{OO})(CNL_1 - CNL_2)_{initial} \quad (2)$$

where [34]

$$S_{OO} = \frac{1}{2}\left(\frac{1}{\varepsilon_1} + \frac{1}{\varepsilon_2}\right). \quad (3)$$

In that expression, ε_1 and ε_2 are the low frequency dielectric constants of the two organic materials.

The CNLs are either calculated using a density-functional theory (DFT) local-orbital approach of the metal/molecule interface in the weak chemistry approximation, or deduced from measurements of energetics of metal/organic interfaces. The theoretical approach, described in detail in [13], calculates the density of states induced in the gap of the semiconductor by the proximity of the continuum of the metal states. The CNL is calculated by integrating the induced local density of states and imposing charge neutrality condition: the total number of electrons distributed in states up to the CNL equals that of the isolated molecule. Such calculations have already been performed for the following organic materials: PTCDA, PTCBI, CBP and CuPc [13,14]. In cases where the CNLs were not calculated, they were deduced from the measured position of the Fermi level at interfaces between the organic material and metals with different work functions using

$$E_F - CNL = S_{MO}(\Phi_M - CNL), \quad (4)$$

where S_{MO} is the metal–organic semiconductor interface parameter, Φ_M is the metal work function, and E_F is the position of the Fermi level at the interface, all three quantities measured in a series of experiments on metal/organic interface energetics [3,6,8]. All levels are referred to the vacuum level (E_{vac}). The positions of the CNLs with respect to E_{vac}, along with the HOMO and LUMO edges of the organic material are given in Table 2.

The fundamental assumption behind this application of the CNL approach to OO systems is that the CNL, calculated (or measured) for MO interfaces, remains a meaningful and representative energy marker for OO heterojunctions. Strictly speaking, the CNL depends on the electronic structure of the (organic) semiconductor, on the electronic density of states of the metal, and on the geometry of the metal/semiconductor interface, and the assumption of a CNL independent of the metal has not been confirmed by specific calculations of the electronic structure of OO interfaces. Yet, the validity of this assumption is supported by the argument that the position of calculated CNLs at interfaces between various organic materials and gold is found to be nearly independent of the metal/organic interaction strength. This is verified in particular by calculating the IDIS and CNL at the metal/organic interface for different distances between the interface molecule and the outer metal atomic plane. The magnitude of the density of states induced in the organic gap, in particular around the CNL, is found to depend strongly on this interaction [13], but the position of the CNL does not. In that sense, the CNL plays the role of an intrinsic level of the organic material, nearly independent of the metal on which it is deposited.

Finally, the dielectric constants of the materials, which are needed to calculate the screening parameter S_{OO}, are generally not known but are evaluated as follows. ε(PTCDA) was measured and is known to be ~1.9 [35]. Furthermore, ε_1 is inversely proportional to the square of the energy gap of the material. Using the gap of the organic materials determined via UPS/IPES, an evaluation of ε relative to that of PTCDA becomes possible (Table 2). S is found to be of the order of 0.6 for most of the compounds studied here (much larger than the values found for inorganic heterojunctions where $\varepsilon \sim 10$ and $S \sim 0.1$). Using these values and the calculated or deduced CNL positions, the above equation for Δ leads to specific predictions of sign and magnitude of the OO heterojunction dipoles, and thus of the molecular level alignment for these interfaces. Calculated and measured OO heterojunction dipoles are compared in Table 1. The signs always agree, and the agreement between the absolute values is reasonably good. The largest discrepancy is 0.16 eV for the bathocuproine (BCP)/PTCBI pair, which is close to the 0.1 eV experimental uncertainty on measurements of interface dipoles.

The results on interface dipoles presented in Table 1 are consistent with the fact that the organic materials investigated here are wide band gap ($E_g \geqslant 2.5$–3 eV), low dielectric constant materials with very few free charge carriers. At interfaces between wide gap (nearly insulating) materials, little charge exchange is expected and the realignment of energy levels is small. This is to be contrasted with interfaces involving metals, where the presence of a large reservoir of free charges allows charge exchange and screening

of the initial difference between the work function and charge neutrality levels of the materials, leading to large dipole values.

Having achieved better understanding and prediction of simple OO interfaces using the concepts of alignment of CNLs, we turn to the experimental observation that p-doping one of the organic constituents of the heterojunction leads to the formation of a large interface dipole accompanied by a commensurate modification of molecular level offsets at the interface [28]. We use the concept of CNL and modification of the electronic structure of the doped organic material to explain the new situation.

3.2. Doped OO heterojunctions

3.2.1. Basic experimental

The energy diagrams of several heterojunctions formed by deposition of an electron transport material (ETM), i.e. BCP or CBP, on an undoped or doped hole-transport material (HTM), i.e. α-NPD or ZnPc, are shown in Fig. 4(a) and (b), respectively. In all cases, doping is done by co-evaporation of the HTM with F_4-TCNQ, and the doping level is indicated. These diagrams of heterojunction energetics lead to several important points. First, none of the four undoped heterojunctions displays a significant interface dipole, in line with the majority of OO interfaces, as mentioned above. Note that the IDIS/CNL model predicts (Table 1) very small dipoles for α-NPD/BCP (−0.12 eV) and for CuPc/CBP (0.09 eV), in agreement with the experimental data. CuPc has nearly the same electronic structure (DOS, energy gap, ionization energy, electron affinity) as ZnPc and is therefore relevant in this comparison. Second, three of the four doped heterojunctions exhibit a significant dipole magnitude (0.5–0.9 eV). Note that the sign of the dipoles is incompatible with cross-doping. Indeed, p-doping of the ETM by diffusion of F_4-TCNQ from the HTM would lead to a shift of the ETM molecular level structure, and thus an interface dipole, in opposite direction. Third, the dipole is not induced by a movement of the Fermi level only. In the experiment described in Fig. 5, the position of the Fermi level in the α-NPD/BCP heterojunction is moved by nearly 1 eV by substituting a low work function metal, i.e. magnesium (Mg), for gold (Au), as the substrate [28]. The interface dipole remains negligible. Fourth, like for undoped OO heterojunction, the molecular level offsets and dipole remain unchanged upon reversal of the deposition sequence, indicating that the measured interface electronic structure is specific to the heterojunction and not affected by fabrication, i.e. by the deposition sequence. Finally, the position of E_F in the energy gap of the undoped ETL remains at a specific position with respect to the HOMO or LUMO, independent of the doped HTL it is deposited on: E_F is 2.26 eV above the BCP HOMO, whether BCP is on doped α-NPD or doped ZnPc, and E_F is 1.60 eV above the CBP HOMO, whether CBP is on doped α-NPD or doped ZnPc. The difference between the interface dipoles at these heterojunctions just compensates for the difference between the work functions of the doped HTLs.

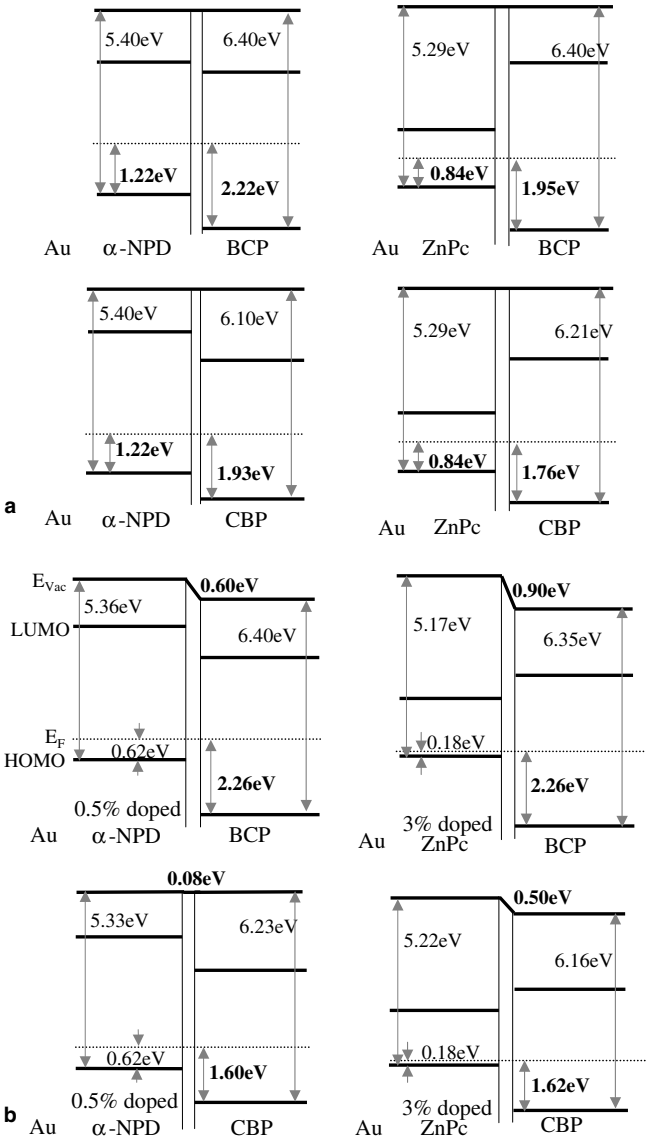

Fig. 4. Electronic structures of four organic HTM/ETM heterojunctions, α-NPD/BCP, ZnPc/BCP, α-NPD/CBP and ZnPc/CBP with (a) undoped HTM and (b) doped HTM (after [28]).

3.2.2. Analysis of the doped heterojunction data using the IDIS model

Before getting to the specific issue of the change in molecular level alignment and interface dipole upon doping of one of the two organic materials, we briefly consider one of the points made in the previous paragraph. The fact that the energetics of an OO interface remain independent of the deposition sequence is a fairly general property of organic/organic heterojunctions [25,26]. Unlike inorganic heterojunctions, where arrays of strong inter-atomic covalent bonds across the interface usually exhibit defects related to the kinetics or to the thermodynamics of growth sequence, the organic heterojunctions considered here

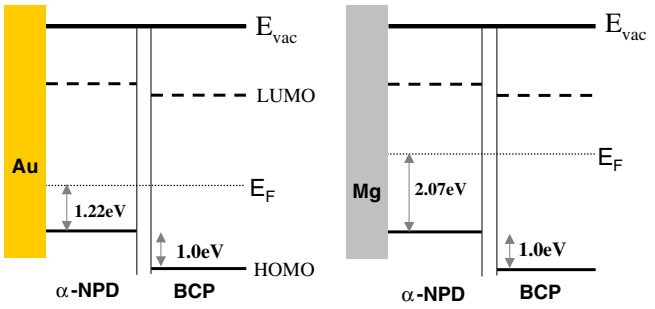

Fig. 5. Electronic structure of the (undoped) α-NPD/CBP heterojunction with (a) Au and (b) Mg substrate. The ~1 eV Fermi level movement due to substrate substitution induces no change in molecular level alignment at the heterojunction (after [28]).

exhibit interfaces with van der Waals-intermolecular bonding between closed-shell molecules that, by and large, are free of electronically active defects. Unless molecular interdiffusion or cross-doping occurs and dominates the electronic structure of the interface, the energetics of the doped OO heterojunctions mentioned above are not expected to exhibit differences based on deposition sequence. This is confirmed by experiments on transitivity in molecular level alignment and equality of interface energetics under reversal of deposition sequence, which have been reported elsewhere for undoped [26,27] and doped [28] interfaces.

The model that requires alignment of the CNLs of the two organics across the interface provides an intuitive approach to the change in dipole when one of the two materials, the HTM in this particular case, is doped. Indeed the changes that take place in the electronic structure of the doped material, especially at high doping concentrations, suggest that the position of the CNL changes upon doping, and thus forces a realignment of the molecular levels of the two materials. An extreme case is presented in Fig. 6, which shows in panel (a) the UPS and IPES spectra measured from undoped ZnPc and ZnPc:30% F_4-TCNQ. Panel (b) shows the HOMO and LUMO positions of the host and dopant, respectively, previously determined by UPS and IPES [31,32]. F_4-TCNQ is an efficient p-dopant in ZnPc due to the fact that its LUMO is only ~50 meV above the ZnPc HOMO (the dopant electron affinity is nearly as large as the host ionization energy), leading to an electron transfer from the ZnPc HOMO to the F_4-TCNQ LUMO. The empty states of the dopant overlap therefore with most of the energy gap of the host. In the 30% doping case, the IPES is able to pick up this large density of states, and the UPS/IPES combination shows that the doped material (nearly an alloy) has only a small gap of a few 100 meV near to bottom of the former gap of ZnPc. If the CNL of pure CuPc (and ZnPc) is about 1.7 eV above the HOMO (Table 2), the CNL of this alloy is clearly much closer to the HOMO of the undoped material. The doping concentrations in the experiments presented in Fig. 4 are far below the 30% of Fig. 6, but are large compared to usual doping concentrations in inorganic semiconductors

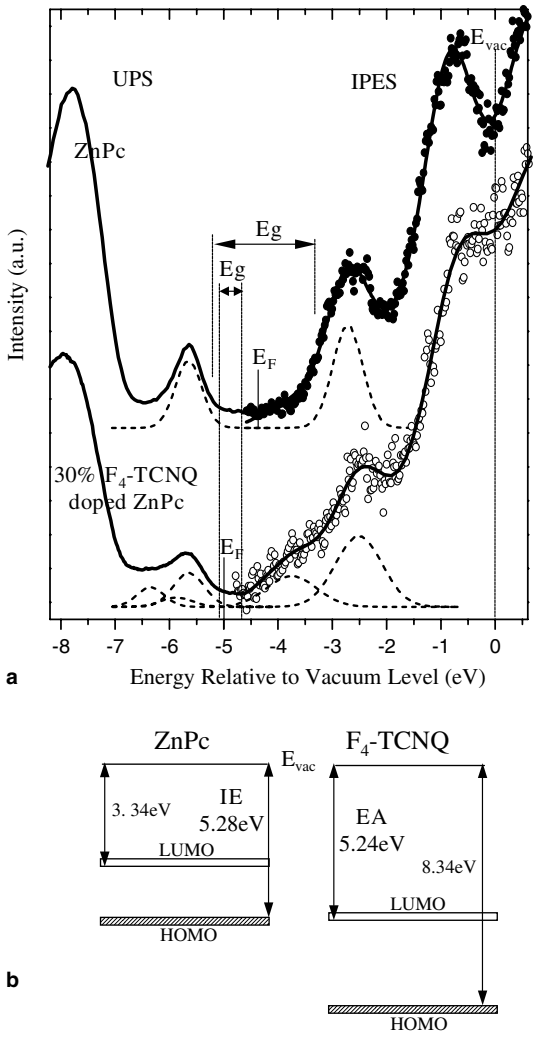

Fig. 6. (a) Combined UPS/IPES spectra of undoped ZnPc (top) and of ZnPc:30% F_4-TCNQ (bottom) films, with the energy position referenced to the vacuum level. Curve fitting of the IPES spectra help locate individual peaks. HOMO and LUMO peaks of the doped film are decomposed and shown in dashed lines. (b) Energy diagram with relative positions of host and dopant molecular levels.

(10^{-4}–10^{-3}%). One can therefore think of the p-doped organic materials of interest here as having a significant density of empty states corresponding to the dopants and overlapping with the upper half of the gap. This, in turn, lowers the CNL of the doped material with respect to that of the undoped one, leading to a realignment of the molecular levels and to the formation of a dipole, as observed in Fig. 4. In addition, the dielectric constant of the doped organic material increases significantly because of the presence of free carriers, and S_{OO} decreases with respect to its value at the undoped interface, according to Eq. (3). The combination of a shifted CNL and smaller S_{OO} leads to a large dipole Δ, according to Eq. (2) and in qualitative agreement with the results of Fig. 4.

A complete calculation of the electronic structure of OO heterojunctions is not possible at this time, as no specific information on the structure of these interfaces is available.

Nevertheless, a quantitative evaluation of the shift in CNL at the interface of the doped organic material can be achieved by examining the doping-induced change in interface energetics at interfaces between that material and metals.

To illustrate this approach, we compare the interface electronic structure of (a) undoped and (b) 0.5% doped α-NPD deposited on Au [33] (Fig. 7). p-doping of the organic semiconductor results in the expected molecular level bending away from the interface, which signals the formation of a depletion region in the organic films. The interface dipole between Au and α-NPD is also seen to decrease as a result of p-doping. Both types of doping-induced changes are observed at other interfaces, such as Au/ZnPc or Mg/ZnPc [31,32]. The change in dipole is related to the change in CNL position via

$$\delta(\mathrm{CNL}) \sim \frac{\delta(\Delta)}{(1 - S_{\mathrm{MO}})}, \tag{5}$$

where S_{MO} is the metal/organic interface parameter defined with Eq. (4). S_{MO} is primarily defined by the metal/molecule interaction and is assumed to remain unchanged in the low doping regime. In the case of α-NPD on Au, the ~0.1 eV change in interface dipole (Fig. 7) and the value of the interface parameter ($S_{\mathrm{MO}} = 0.5$ [8]) translate to a 0.2 eV shift of the CNL position toward the HOMO when the organic material is doped with 0.5% of F_4-TCNQ. Therefore the CNL, referred to the vacuum level of the material, shifts from −4.2 to −4.4 eV. Considering that the dielectric constant of doped α-NPD is large compared to that of the undoped material and taking $\varepsilon(\mathrm{BCP}) \sim 1.4$ (Table 2), Eq. (3) gives a value of $S_{\mathrm{OO}} \sim 0.35$ for the doped α-NPD/BCP interface. Using this value, the new CNL position of α-NPD and the CNL position BCP (Table 2), Eq. (2) yields a dipole $\Delta = (1 - S_{\mathrm{OO}})(\mathrm{CNL}_1 - \mathrm{CNL}_2) = -0.40$ eV. Table 3 summarizes the results obtained with this approach for the interfaces presented in Fig. 4. The agreement with experimental data is fairly good for α-NPD/BCP (−0.40 vs. −0.6 eV) and for α-NPD/CBP (−0.15 vs. −0.1 eV). The results are not as close for the heterojunctions involving the highly doped ZnPc, though they show the correct tendency for the formation of a measurable dipole upon doping and predicts the dipole sign.

Table 3
Comparison between measured and calculated dipoles for the four doped heterojunctions of Fig. 4(b), using the approach (discussed in the text) based on a doping-induced shift of the CNL calculated from the electronic structure of the doped organic/metal interface

	Δ(experiment)	Δ(calculated)
0.5% doped α-NPD/BCP	−0.6	−0.40
0.5% doped α-NPD/CBP	−0.1	−0.15
3% doped ZnPc/BCP	−0.9	−0.5
3% doped ZnPc/CBP	−0.5	−0.2

The agreement obtained with the approach described above is qualitative in nature and does pretend to address the details of the electronic structure of these OO heterojunctions. Nevertheless, it captures in a consistent fashion one of the key physical phenomena that defines molecular level alignment at both MO and OO interfaces. The doping-induced shift in the CNL of the material is extracted from data and equations that pertain to MO interfaces and are independent of the OO heterojunctions analyzed here. It is then applied successfully to describe the doped OO interfaces. The relatively poor quantitative agreement between measured and predicted dipoles for interfaces involving ZnPc is presumably due to an underestimation of the CNL shift in the highly doped (3%) material. It is likely that such a high doping level profoundly affects of the electronic structure of the material, as exemplified with the extreme case of 30% doping discussed above (Fig. 6). The assumption made above that S_{MO} remains unchanged by doping in Eq. (5) also presumably contributes to worsening the agreement between theory and experiment. Taking a CNL position closer to the Fermi level of the material would, in this case, lead to better quantitative agreement than in Table 3. An ab initio calculation of the electronic structure of doped molecular films will be needed to address the problem in a fundamental way.

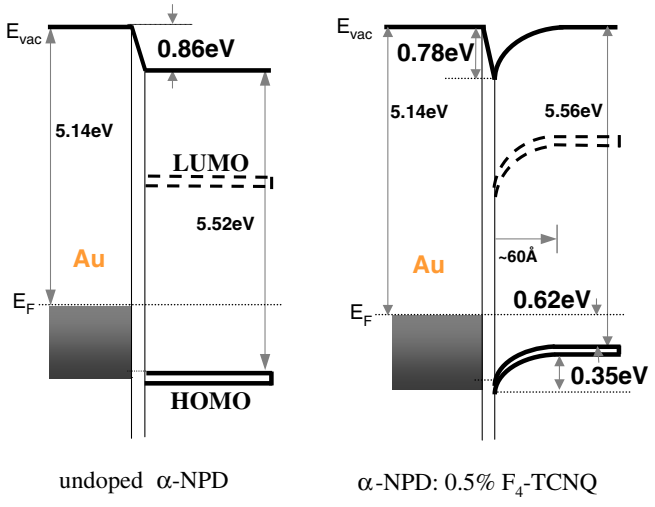

Fig. 7. Energy diagram of the Au/α-NPD interface obtained by UPS as a function of deposition of undoped (left) and 0.5% doped (right) α-NPD.

4. Summary

Using the concept of CNL alignment previously developed for predicting the electronic structure of undoped OO heterojunctions, we present here an ad-hoc model to understand the doping-induced changes in interface dipole at doped heterojunctions. Using experimental results on energy level and dipole shifts induced by doping at MO interfaces, we calculate the doping-induced shifts in CNL position of two specific organic materials, then apply these shifts to recalculate the interface dipole at doped OO interfaces involving these materials. Good qualitative agreement with experiment is obtained. This approach provides the first consistent means of understanding, in an entirely con-

sistent way, the evolution of MO and OO energetics upon electrical doping the organic semiconductor.

Acknowledgments

The Princeton group is grateful for support for this work by the National Science Foundation (DMR-0408589), the Princeton MRSEC of the National Science Foundation (DMR-0213706), and the New Jersey Center for Organic Optoelectronics. The Madrid group acknowledges financial support by the Consejería de Educación de la Comunidad de Madrid, the DIODE network sHPRN-CT-1999-00164d, and the Spanish CICYT under Project No. MAT 2001-0665.

References

[1] H. Ishii, K. Seki, IEEE Trans. Elect. Dev. 44 (1997) 1295.
[2] W.R. Salaneck, S. Stafström, J.L. Brédas, in: Conjugated Polymer Surfaces and Interfaces; Electronic and Chemical Structure of Interfaces for Polymer Light Emitting Devices, Cambridge Univ. Press, Cambridge, 1996.
[3] I. Hill, A. Rajagopal, A. Kahn, Y. Hu, Appl. Phys. Lett. 73 (1998) 662.
[4] H. Ishii, K. Sugiyama, E. Ito, K. Seki, Adv. Mater. 11 (1999) 605.
[5] I.G. Hill, J. Schwartz, A. Kahn, Org. Elect. 1 (2000) 5.
[6] W.R. Salaneck, K. Seki, A. Kahn, J.J. Pireaux (Eds.), Conjugated Polymer and Molecular Interfaces, Marcel Dekker, Inc., New York, 2001.
[7] N.J. Watkins, L. Yan, Y. Gao, Appl. Phys. Lett. 80 (2002) 4384.
[8] A. Kahn, N. Koch, W. Gao, J. Polym. Sci., Polym. Phys. 41 (2003) 2529.
[9] M. Lögdlung, T. Kugler, G. Greczynski, A. Crispin, W.R. Salaneck, M. Fahlman, in: W.R. Salaneck, K. Seki, A. Kahn, J.J. Pireaux (Eds.), Conjugated Polymer and Molecular Interfaces, Marcel Dekker, Inc., New York, 2001, p. 73.
[10] C. Shen, A. Kahn, Org. Elect. 2 (2001) 89.
[11] X. Crispin, V. Geskin, A. Crispin, J. Cornil, R. Lazzaroni, W.R. Salaneck, J.L. Bredas, J. Am. Chem. Soc. 124 (2002) 8131.
[12] P.S. Bagus, V. Staemmler, C. Wöll, Phys. Rev. Lett. 89 (2002) 096104.
[13] H. Vazquez, R. Oszwaldowski, P. Pou, J. Ortega, R. Perez, F. Flores, A. Kahn, EuroPhys. Lett. 65 (2004) 802.
[14] H. Vazquez, F. Flores, R. Oszwaldowski, J. Ortega, R. Perez, A. Kahn, Appl. Surf. Sci. 234 (2004) 107.
[15] V. Heine, Phys. Rev. 138 (1965) A1689.
[16] S.G. Louie, M.L. Cohen, Phys. Rev. B 13 (1976) 2461.
[17] S.G. Louie, J.R. Chelikowsky, M.L. Cohen, Phys. Rev. B 15 (1977) 2154.
[18] C. Tejedor, F. Flores, E. Louis, J. Phys. C 10 (1977) 2163.
[19] F. Flores, C. Tejedor, J. Phys. C 20 (1987) 145.
[20] W. Mönch, in: Semiconductor Surfaces and Interfaces, Springer Verlag, Berlin, Heidelberg, 1993.
[21] H. Vazquez, W. Gao, F. Flores, A. Kahn, Phys. Rev. B 71 (2005) 041306.
[22] R. Schlaf, B.A. Parkinson, P.A. Lee, K.W. Nebesny, N.R. Armstrong, Appl. Phys. Lett. 73 (1998) 1026.
[23] I.G. Hill, A. Kahn, J. Appl. Phys. 86 (1999) 2116.
[24] I.G. Hill, A. Kahn, J. Appl. Phys. 86 (1999) 4515.
[25] I.G. Hill, D. Milliron, J. Schwarz, A. Kahn, Appl. Surf. Sci. 166 (2000) 354.
[26] A. Rajagopal, A. Kahn, Adv. Mater. 10 (1998) 140.
[27] A. Rajagopal, C.I. Wu, A. Kahn, J. Appl. Phys. 83 (1998) 2649.
[28] W. Gao, A. Kahn, Appl. Phys. Lett. 82 (2003) 4815.
[29] C.I. Wu, Y. Hirose, H. Sirringhaus, A. Kahn, Chem. Phys. Lett. 272 (1997) 43.
[30] I.G. Hill, A. Kahn, Z.G. Soos, R.A. Pascal Jr., Chem. Phys. Lett. 327 (2000) 181.
[31] W. Gao, A. Kahn, Appl. Phys. Lett. 79 (2001) 4040.
[32] W. Gao, A. Kahn, Org. Elect. 3 (2002) 53.
[33] W. Gao, A. Kahn, J. Appl. Phys. 94 (2002) 359.
[34] J. Tersoff, Phys. Rev. B 32 (1985) 6968.
[35] Z. Shen, S.R. Forrest, Phys. Rev. B 55 (1997) 10578.